Effects of the homogeneous current of ECE theory

Horst Eckardt

Alpha Institute for Advanced Study (A.I.A.S),
www.aias.us, www.atomicprecision.com
HorstEck@aol.com

Abstract

xxx.

1 Introduction

xxx.

2 Numerical method for solving the ECE field equations

See Numerical Note 2

3 Tests of the divergence term

Equations () have been solved numerically as described in section 2. First the effect of the grad div term will be investigated in some detail, because such terms play an importand role in the resonance equations of ECE theory []. We omit the gradient and concentrate on the divergence of the fields. For the investigation, a “conventional” configuration has been chosen with a given inhomogeneous current J, no homogeneous current has been assumed. Thus the ordinary Maxwell equations are obtained from eq. (), besides of the polarization index which is not considered further in this paper.

The geometry chosen is a cube with empty-space boundary conditions E=H=0. In the center there is a conducting rod as shown in Fig. 3a,b with a current density from left to right in parallel to the axis. Figs. 1 and 2 show a vertical cut. The current density creates a magnetic field around the conductor as shown in Figs. 1a,b. In all figures the lines of constant field strength (comparable to equipotential lines) are shown. For a circular magnetic field these are in parallel with the field lines.

In Fig. 1a the result is shown where the divergence term has been omitted in the calculation, in Fig. 1b the term has been included. Both calculations were carried out to convergence (to a precision of 10^{-5}). The maximum field value is about 3.5 A/m for a current density of 1000 A/m^2. The effect of the divergence term is minimal due to the fact that the H field is divergence free. Only in the border region a better adoption to the boundary geometry is visible for the calculation including the div term.

The situation is quite different for the electric field. This field occurs because we have carried out an AC calculation (frequency of 10 kHz). The E field is phase shifted by 90 degrees and relatively weak (less than 0.1 V/m). In the case of DC it would vanish completely. In this calculation we have not regarded the conductivity of the rod. Therefore there is no E field present in the DC case.

Fig. 2 shows a significant effect of the div term. Without this term (Fig. 2a) there is no electric source visible at both ends of the conducting rod. With the div term included, the front surfaces act as field sources as expected.

The effect of the divergence is further analysed in Fig. 3. in 3a, the fields were calculated self-consistently without the div term, and the quantity div E was calculated in one additional step after the calculation had converged. This can be considered as some kine of “perturbation theory”. The result has to be compared to the div E of the fully self-consistent calculation (Fig. 3b). The results are qualitatively similar, looking something more relaxated in the second case. However, the values are about an order of magnitude too small in the perturbational approach. This shows the importance of correct numerical treatment of the divergence term.

Besides the divergence of the electric field, also the divergence of the magnetic field has been examined (Fig. 4), again calculated within the perturbational approach (4a) and the fully self-consistent correct way (4b). In both cases the central region of the rod is divergence-free as required, but near to the borders of the definition volume a significant divergence occurs. This has alternating signs and shows up the symmetry of the arrangement (some iso surfaces are shown additionally in Fig. 4). Obviously there is a tendency towards eigen value solutions of the cube in this region. However, the H field values are very small there so that this has no significant effect on the results as can be seen by comparison with

Fig. 1. This finding is in accordance with the prediction made in [1st num. paper]. In addition, there is a dependence on the discretization. Enlarging the grid from 50x50x50 to 100x100x100 leads to a shift of the divergence region to the borders, roughly in the same way as going from Fig. 4b to 4a. The results in the central region remain stable.

4 Effects of the homogeneous and inhomogeneous current

In the following the effects of the homogeneous and inhomogeneous current are described. A geometric configuration has been chosen similar to that described in section 3, but the rod has been filled by a homogenous current, an inhomogeneous current or both.

From eq. () it can be seen that both equations for E and H are fully symmetric in form. This has consequences to the form of the fields when a current is predefined as in these calculations. While the inhomogeneous current creates a primary magnetic field and a secondary electric field, a homogeneous current does the reverse. This is unusal for the electrical engineer but clear from the theory. The calculation does confirm this. Figs. 5a,b are either the lines of constant magnetic field for an inhomogeneous (charge) current or the lines of an electric vortex field for a homogeneous current. The chosen values of 1000 A/m^2 or 1000 V/m^2, respectively, lead to the same numerical maximum field values of about 3.5 A/m or 3.5 V/m, correspondingly.

As the charge current leads to a secondary electric field, the homogeneous current creates a secondary magnetic field. Interestingly, this secondary field is a source field (see Fig. 6a). So an alternating homogeneous current (for example created in a dielectric by resonance) leads to magnetic monopoles. They are quite weak in strength because it is the secondary field of the current density, and even weaker than in the case of a charge current, because the factor ε_0 in eq. () is numerically smaller than μ_0. The source terms are therefore weighted differently.

The divergence of the secondary source fields has been shown in Fig. 7a,b. This is basically identical to that of Fig. 3b.

It has further to be noted that the secondary fields are shifted from the primaries by a phase of $\pi/2$. The results are summarized in Table 1. Combining both types of currents leads to a superposition of both types of fields, so a rotational magnetic as well as a rotational electric field are present at the same time. When both currents have a phase difference of $\pi/2$, the primary field of one current dominates the secondary field of the other in each case. Then there are only two rotational primary fields. The occurrence of rotational electric fields may be a hint for the experimentalists that there is a homogeneous resonance current present.

Current type	Field	$\varphi = 0$	$\varphi = \pi/2$
$J \neq 0$	**E**		secondary source field
	H	rotational field	
$j \neq 0$	**E**	rotational field	
	H		secondary source field (very weak)

$J \neq 0$, $j \neq 0$	**E**	rotational field	secondary source field
	H	rotational field	secondary source field (very weak)
$J \neq 0$, $j \neq 0$, $\varphi(j) = \pi/2$	**E**		rotational field
	H	rotational field	

Table 1. Field types of inhomogeneous and homogeneous current.

5 Results for an inhomogeneous current within a coil

As a more practical example we consider a coil with an internal dielectric. The coil generates a conventional magnetic field, and at resonance the internal rod produces a homogeneous current. The geometry and the conventional lines of constant magnetic field are shown in Fig. 8a,b.

The secondary electric field of the coil is concentrated in the inner region and in part in the outer region (Fig. 9a). In the conducting material itself there is no significant field. This does not mean that the coil is free of electric fields. We have not modelled here the field which generates the current. We would have to introduce a conductivity term in the equations () for this. Here we concentrate on the additional effects enhancing or diminishing the current.

As described in the previous section, “switching on” the homogeneous current of comparable strength as the charge current leads to a strong electric field around the rod. As can be seen from Fig. 9b, the field is most significant in the coil region, leading to an enhanced movement of the charge carriers. An additional voltage is present in the coil due to the electric field of the homogeneous current. According to the entries in Table 1, the fields are in phase with the generating currents. The device may not behave as a conventional inductive element, where voltage and ccurrent are shifted by a phase difference of $\pi/2$.

6 Conclusions

Significant effects of the homogeneous and inhomogeneous current of ECE theory have been described and verified by numerical calculations. There is a strong symmetry between both types of currents as well as both types of fields which is not present in Maxwell theory. In the latter the current is a pure charge current and introduced phenomenologically, while in ECE theory both currents are directly derived from Cartan geometry. Neverveless, in ECE theory the currents can be considered to be predefined and chosen for input in a numerical calculation.

The results show that the divergence term cannot be neglected as soon as source-like fields play a role. When omitting this term, qualitiative behaviour is retained which may give a justification for certain approximations made in resonant ECE theory for deriving analytical solutions [].

The symmetry of the ECE equations for both the E and H field leads to field configurations hitherto unknown. For example static rotational electric fields are possible due to a static homogeneous current. Conversely, resonant currents may be discovered by finding such unusual field configurations in experiments. As a special example, the electric current through a coil can be greatly enhanced by such effects.

In this article we had to let open the question how such resonances can be created. However, the fundamental existence of them is ensured by the resonance solutions of ECE theory []. Therefore our next steps of numerical work will go into this direction.

7 Acknowledgement

The author is grateful for many encouraging discussions within the AIAS group which promoted the inception of this work.

8 References

[1] M. W. Evans, Generally Covariant Unified Field Theory (Abramis, 2005, softback), volume one. Ibid., vol. 2 in press, vol. 3 in preparation (preprints of vols. 2 and 3 available on www.aias.us and www.atomicprecision.com).

[2] M. W. Evans, Resonance Solutions of the ECE Field Equations (2006, ref. [1], vol. 3, pp. 109-128; see also preprint 52 on www.aias.us and www.atomicprecision.com).

[3] M. W. Evans, Resonant Counter Gravitation (2006, ref. [1], vol. 3, pp. 129-151; see also preprint 53 on www.aias.us and www.atomicprecision.com).

[4] M. W. Evans, First and Second Order Aharanov Bohm Effects in the Evans Unified Field Theory (2005, ref. [1], vol. 2, pp. 17-26; see also, preprint 27 on www.aias.us and www.atomicprecision.com).

[5] L. Lehner, Numerical relativity: a review, Class. Quantum Grav. 18 (2001) R25–R86.

[6] J. B. Marion, S. T. Thornton, Classcial Dynamics of Particles ans Systems (Saunders College Publishing, Fort Worth, Philadelphia), fourth edition 1995, pp. 125-131.

[7] J. D. Jackson, Classcial Electrodynamics, Third Edition (John Wiley and Sons, 1998), p. 295.

[8] C. Cuvelier, A. Segal, A. A. van Steenhoven, Finite Elemt Methods and Navier-Stokes Equations (1986, D. Reidel Publishing Company Dordrecht), p. 26.

[9] http://mathworld.wolfram.com/SuccessiveOverrelaxationMethod.html.

[10] O. Kolditz, Computational methods in environmental Fluid mechanics. (2002, Graduate Text Book, Springer Science Publisher, Berlin).

[11] Ref. [8], p. 329.

[12] U. Trottenberg, C. Oosterlee, A. Schüller, Multigrid (2001, Academic Press, London).

[13]

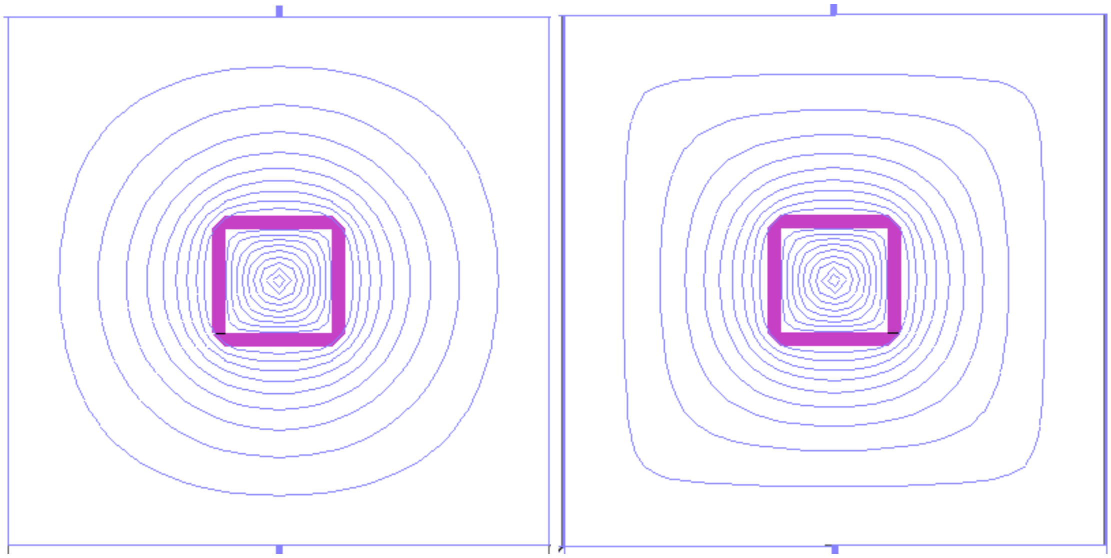

Fig. 1 a,b: Magnetic field.

a: Magnetic field without div term, b: Magnetic field with div term.

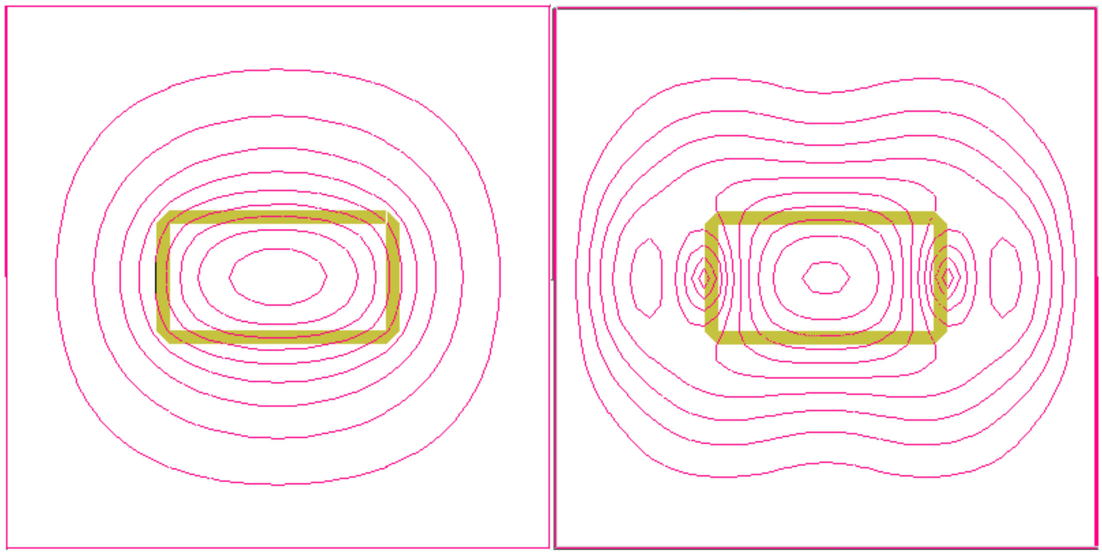

Fig. 2 a,b: Electric field.

a: Electric field without div term, b: Electric field with div term.

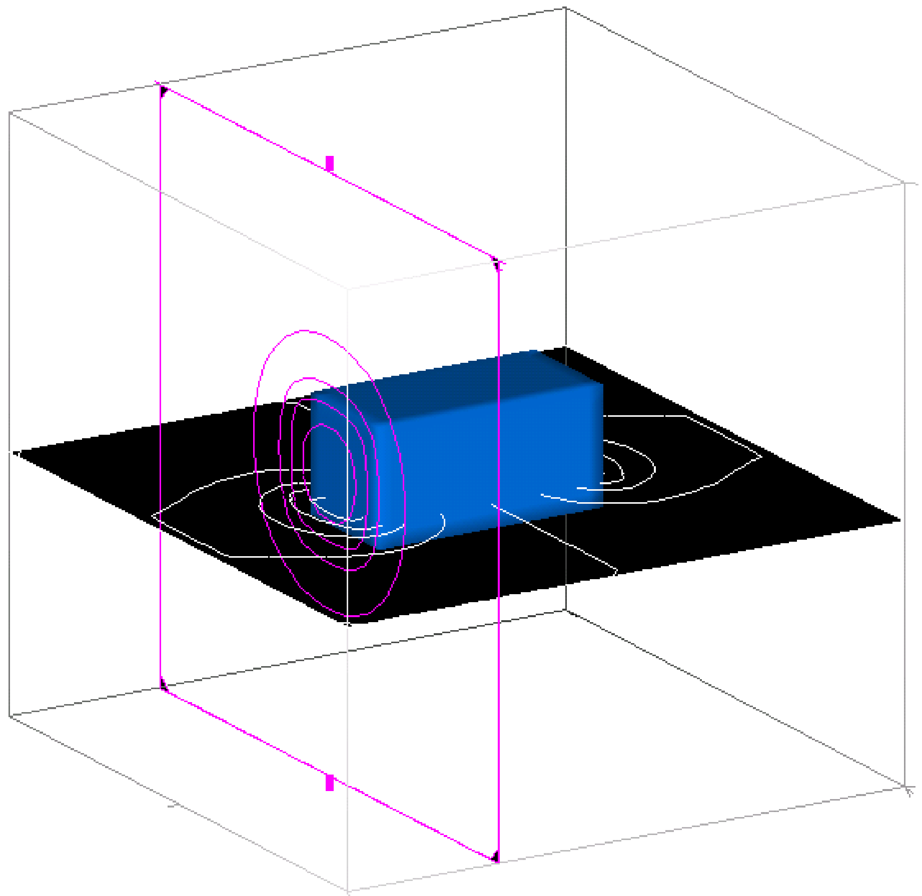

Fig. 3a: Divergence of E field determined by perturbational. calculation.

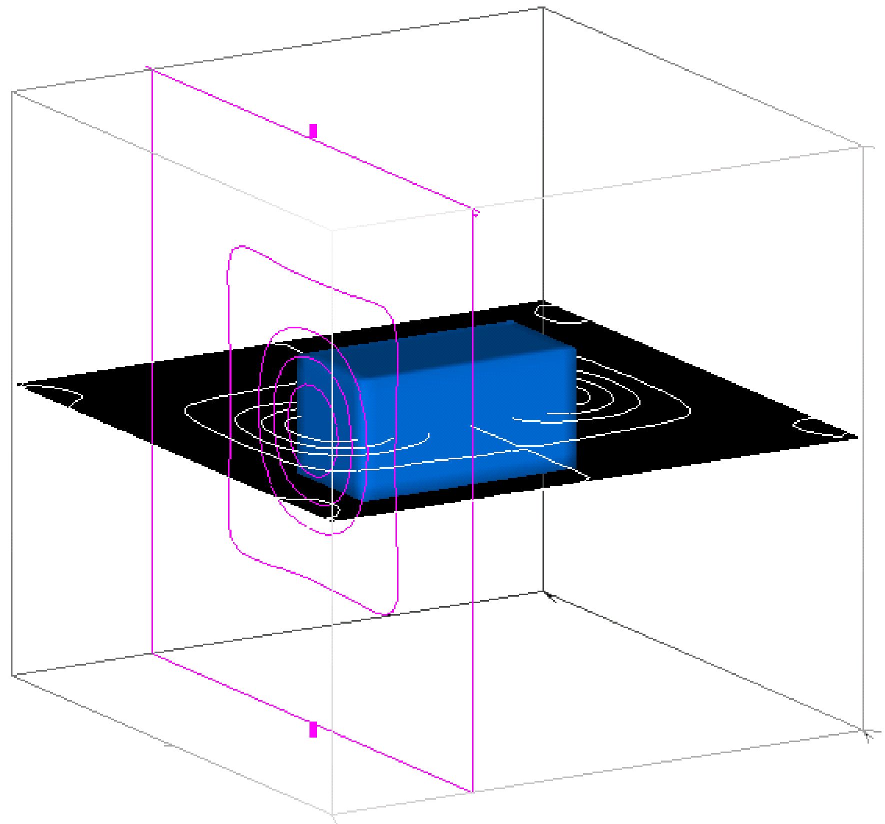

Fig. 3b Divergence of E field determined by self-consistent calculation

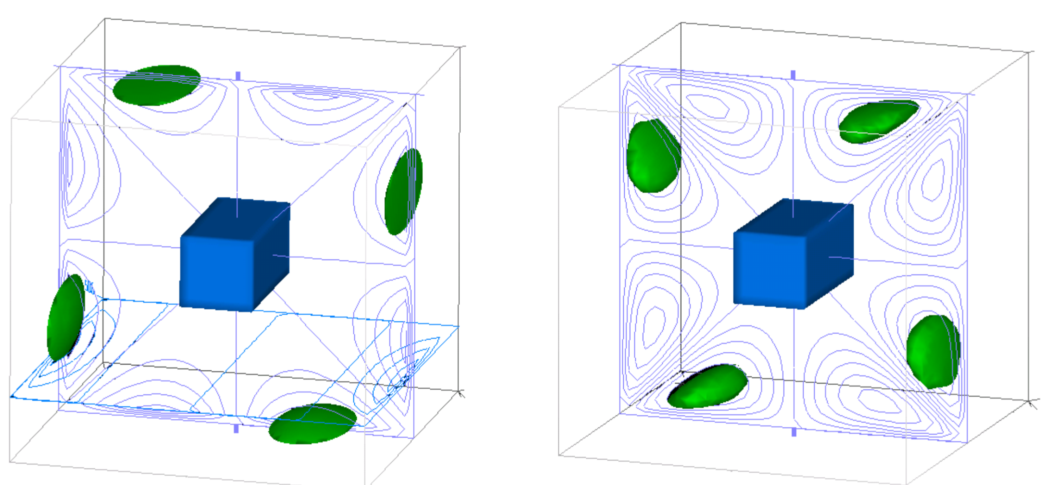

Fig. 4a,b: Divergence of H field with Iso surfaces.

a: Divergence of H field determined by perturbational calculation, b: Divergence of H field determined by self-consistent calculation

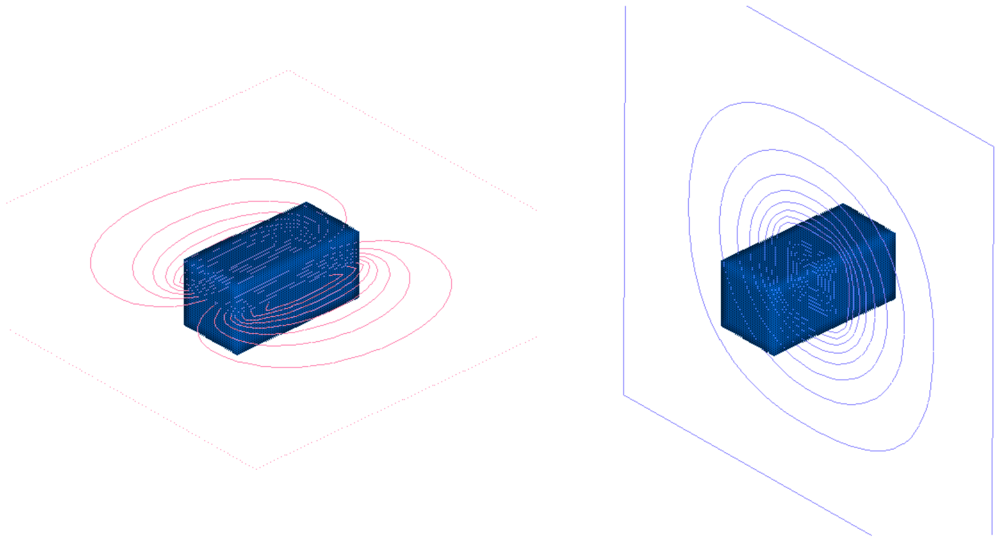

Fig. 5a,b: Magnetic primary field of inhomogeneous current, quantitatively identical to primary electric field of homogeneous current.

a: Fields in x-y plane, b: Fields in y-z plane.

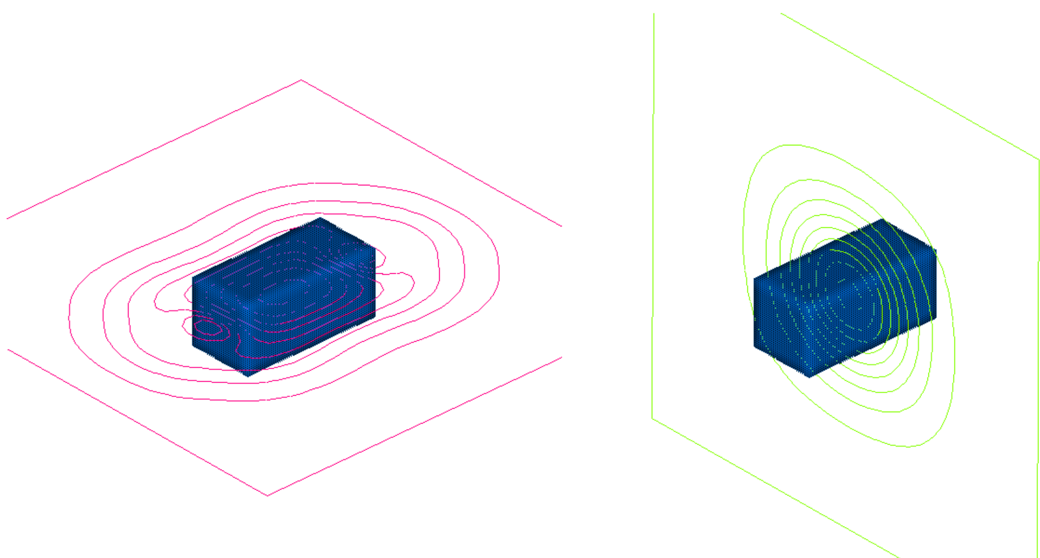

Fig. 6a,b: Electric secondary field of inhomogeneous current, qualitatively identical to magnetic secondary field of homogeneous current.

a: Fields in x-y plane, b: Fields in y-z plane.

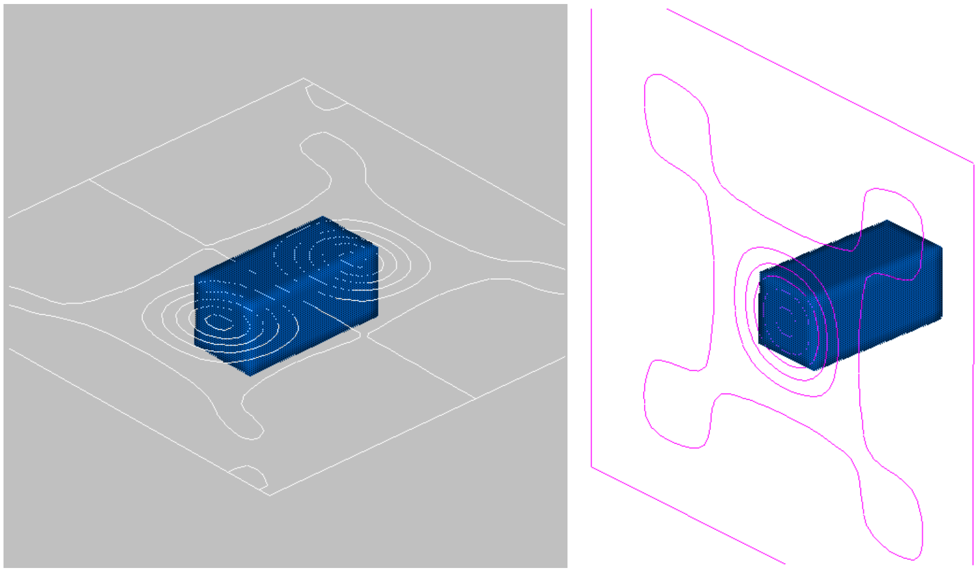

Fig. 7a,b: Divergence of secondary fields, qualitatively identical to both types of current.

a: Divergence in x-y plane, b: Divergence in y-z plane.

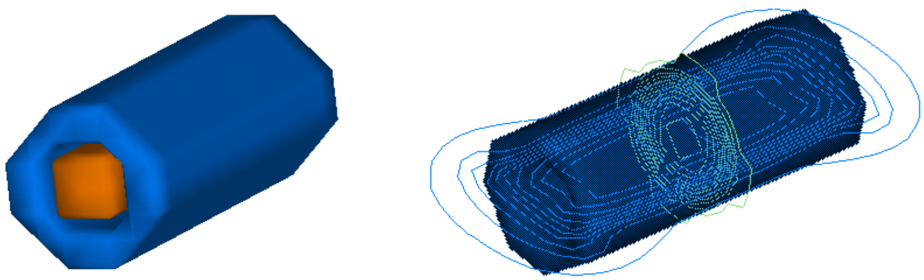

Fig. 8a: Coil with internal conductor for homogeneous current (dielectric).

Fig. 8b: Magnetic Field of coil without homogeneous current.

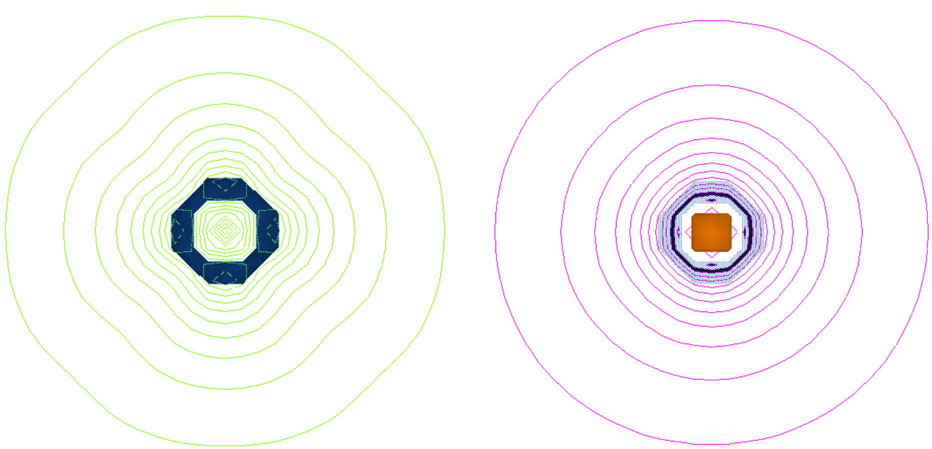

Fig. 9a: Secondary electric field of inhomogeneous current (no field in coil).

Fig. 9b: Primary electric field of homogeneous current (strong field enhancement in coil).